

1998

# CO<sub>2</sub> Heat Pump Water Heater: Simulation and Test Results

R. Rieberer

*Graz University of Technology*

H. Halozan

*Graz University of Technology*

Follow this and additional works at: <http://docs.lib.purdue.edu/iracc>

---

Rieberer, R. and Halozan, H., "CO<sub>2</sub> Heat Pump Water Heater: Simulation and Test Results" (1998). *International Refrigeration and Air Conditioning Conference*. Paper 400.

<http://docs.lib.purdue.edu/iracc/400>

This document has been made available through Purdue e-Pubs, a service of the Purdue University Libraries. Please contact [epubs@purdue.edu](mailto:epubs@purdue.edu) for additional information.

Complete proceedings may be acquired in print and on CD-ROM directly from the Ray W. Herrick Laboratories at <https://engineering.purdue.edu/Herrick/Events/orderlit.html>

# CO<sub>2</sub> HEAT PUMP WATER HEATER: SIMULATION AND TEST RESULTS

René Rieberer and Hermann Halozan  
Institute of Thermal Engineering, Graz University of Technology  
Inffeldgasse 25, A-8010 Graz, Austria  
Phone: ++43 316 873-7311 (Fax: -7305)  
E-mail: rieberer@iwt.tu-graz.ac.at

## ABSTRACT

Within the EU JOULE Project COHEPS, the Institute of Thermal Engineering is investigating CO<sub>2</sub> as working fluid for heat pumps. One main task is the development of a steady-state design model for heat pump water heaters and the verification of the model using measurements from a prototype.

Based on calculations with the heat pump design model HPSTAT, a prototype of a brine to water heat pump with a heating capacity of about 15 kW has been designed and constructed. First measurements with this prototype have been carried out already. Comparisons of calculated and measured values have shown that the simulation model describes the reality very well.

Simulations and measurements confirm that the heat transfer coefficient of CO<sub>2</sub> is very high, and the effect of pressure drop is very low. This results in compact and inexpensive heat pump components. However, no reliable correlation for the two-phase heat transfer coefficient in the evaporator has been found until now.

## 1 INTRODUCTION

Within the EU JOULE Project COHEPS, the Institute of Thermal Engineering is investigating CO<sub>2</sub> as working fluid for heat pumps. The trans-critical CO<sub>2</sub> cycle - the Lorentzen cycle - is well suited for applications with a limited heat-sink and an unlimited heat-source. This is the case in heat pump water heaters (HPWH), air heating systems, and convective dryers (Neksa, 1997; Rieberer, 1997a).

In the case of a limited heat-sink, heat input results in a temperature glide of the heat-sink medium. If CO<sub>2</sub> (R-744) is used as refrigerant, in a HPWH the exergetic losses in the 'condenser' (single-phase cooler) operating under trans-critical conditions become smaller than in a conventional sub-critical condenser due to a better adaptation of the refrigerant temperature to the heat-sink temperature. Furthermore, the compressor pressure ratio by using CO<sub>2</sub> is low, the compressor efficiency becomes high. The compressor outlet temperature is low, this allows maximum heat-sink outlet temperatures higher than 80°C without any problems with the lubricant. The high pressure level results in high densities and therefore in compact heat pump components. Additionally, CO<sub>2</sub> is a 'natural' fluid, and it is a safety refrigerant.

A disadvantage of the Lorentzen cycle is that the COP drops remarkably with rising heat-sink inlet temperatures. This means for a HPWH that reheating of hot water cooled down by insulation losses and circulation losses has to be minimized by proper system design. Since for achieving the maximum COP an optimum pressure at heat-rejection exists, a high-pressure control has to be used.

In order to develop highly efficient CO<sub>2</sub> heat pumps, a reliable simulation program is needed. The steady-state design model HPSTAT is being developed to solve this 'new' problem for HPWHs. However, there is a lack of knowledge regarding models for CO<sub>2</sub> heat transfer and pressure drop. To solve these uncertainties, a HPWH test rig with a heating capacity of about 15 kW has been designed and constructed, it is in operation since autumn 97. This paper presents the most important results gained.

## 2 HPWH TEST RIG

The main components of the test rig at the Institute are shown in Figure 1. They are an open-type reciprocating compressor, a counter-flow 'condenser', an evaporator, an internal heat exchanger (IHX), an accumulator, and a throttling valve. All heat exchangers used in the test rig are of coaxial (tube in tube) type, they are made of copper. Figure 1 also shows a CO<sub>2</sub> cycle in the temperature-entropy (t-s) diagram. The heat-sink as well as the heat-source are indicated by dotted lines.

The compressor lifts the refrigerant from a sub-critical to a trans-critical pressure (1-2). In the ‘condenser’ heat is rejected - in contrast to a conventional heat pump - with a continuous temperature glide (2-3). In the IHX the high-pressure side becomes sub-cooled (3-4) and the suction gas super-heated (7-1). The expansion device throttles the pressure to the sub-critical evaporation pressure (4-5). In the evaporator heat is absorbed from water or brine (5-6). After the evaporator an accumulator is arranged (6-7).

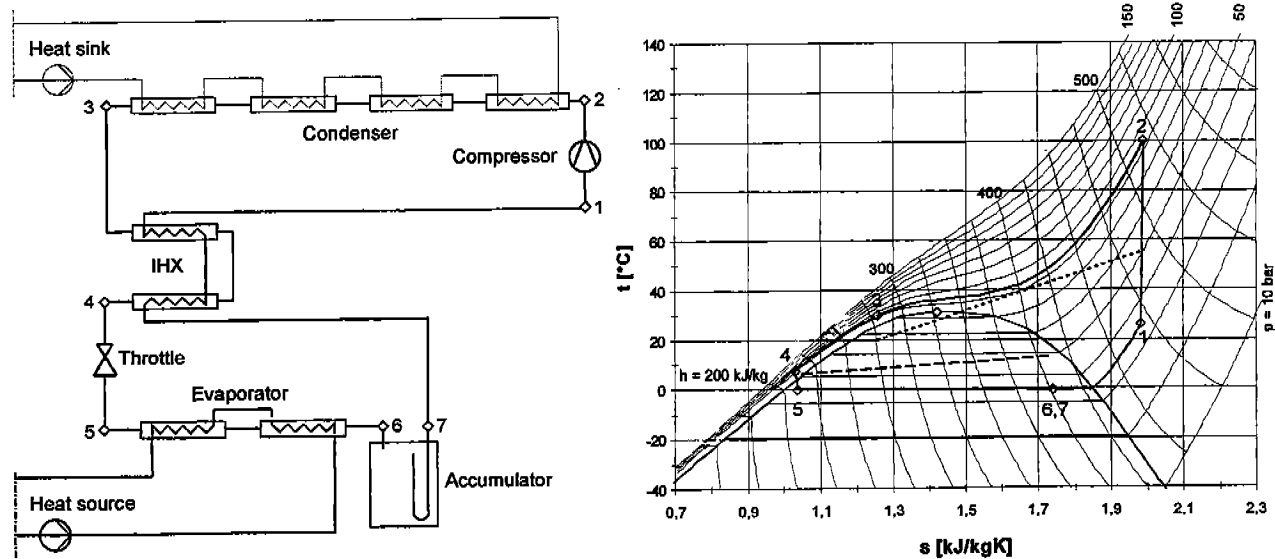


Figure 1: HPWH test rig and a trans-critical process in the t-s diagram

The ‘condenser’ consists of four straight sections arranged in series, each with a length of 3.9 m. The CO<sub>2</sub> flows in the inner tube which has an inner diameter of 7.8 mm. The heat-sink (water) flows in the annulus. The outside surface of the inner tube is finned to increase the heat transfer rate (unfinned outside diameter of the inner tube 9.65 mm, finned diameter 12.6 mm, heat transfer surface enlargement factor by the fins 4.1).

The principle design of the evaporator is similar to that of the ‘condenser’. It consists of two straight sections each with a length of 5.8 m. The CO<sub>2</sub> flows in the inner one of the tubes arranged coaxially ( $\varnothing_{\text{inside}} 15 \times 1.5$  mm,  $\varnothing_{\text{outside}} 28 \times 1$  mm); the heat-source (water or brine) flows in the annulus. In the wall of the inner tube nickel/chrome-nickel thermocouples (Type K) are embedded in order to carry out heat transfer measurements. Two thermocouples are used at each location, one at the top and one at the bottom, to determine a possible separation of the liquid and gaseous CO<sub>2</sub> phase.

The accumulator is arranged after the evaporator. It avoids a deficit of refrigerant in the cycle, it is a refrigerant store to cover possible losses due to leakage, and it acts as a liquid separator. The pressure in the accumulator is given by the evaporation temperature and therefore by the heat-source temperature. In steady-state operation always an equilibrium between the liquid and gaseous phase exists. The line to the IHX is connected to a U-tube (see Figure 5) which has a hole with a diameter of 2 mm on the bottom. Through this hole a mixture of liquid CO<sub>2</sub> and oil is sucked from the gaseous CO<sub>2</sub> which enters the U-tube (diameter 10 mm) on the top. This system secures the oil-return to the compressor.

An IHX can be helpful for reducing the optimum pressure in the ‘condenser’ as well as the influence of deviations from the optimum pressure on the COP. It also avoids compressor damage due to liquid compression. The design is similar to that of the ‘condenser’; the inner tube - in which the high-pressure CO<sub>2</sub> flows - is the same as used for the ‘condenser’. The low-pressure CO<sub>2</sub> flows in the annulus. The outside tube has an inner diameter of 20 mm. Two sections of tubes are arranged in series. The heat is exchanged in counter-flow.

The compressor is a two-cylinder reciprocating refrigeration compressor, modified and optimized with respect to the pressures required for trans-critical CO<sub>2</sub> cycles. The volumetric flow rate is 1.81 to

5.43 m<sup>3</sup>/h, corresponding to the speed range of 500 to 1500 rpm. The maximum working pressure is 130 bar. It is driven by an inverter-driven motor.

The throttling device was a manually operated needle-valve, now it has been changed to an automatically working valve developed especially for CO<sub>2</sub>. The pressure at throttling inlet is the pressure at ‘condenser’-inlet, reduced by the pressure drop in the ‘condenser’. This pressure drop is - compared to the absolute pressure level - very small. The pressure at throttling outlet is given by the evaporating pressure.

The prototype is equipped with thermocouples and pressure transmitters for measurement of temperature and pressure at the beginning and the end of each section of the heat exchangers. A Coriolis mass flow meter is used for measuring the CO<sub>2</sub> mass flow through the cycle. The measurement of speed and torque of the compressor is offered by the motor.

### 3 SYSTEM SIMULATION AND VERIFICATION

This chapter deals with the calculation models used in the steady-state simulation program HPSTAT and their verification by means of the test rig. In the following sections, the heat transfer coefficients ( $\alpha$ ), and overall heat transfer coefficients ( $k$ ) are based on the (unfinned) outside diameter of the inner tube. All calculations are carried out with the LMTD method. The heat transfer coefficients on the water side are verified by measurements with an accuracy of about  $\pm 7\%$ .

#### 3.1 ‘Condenser’ (single-phase cooler)

In a CO<sub>2</sub>-HPWH heat rejection takes place near the critical point of the refrigerant (31.1°C / 73.8 bar). The peak of the Prandtl number near this point results in a heat transfer coefficient which varies strongly with the tube length. Several models for heat transfer and pressure drop in sub-critical single-phase flow are available in literature. In the case of trans-critical single-phase flow, specific CO<sub>2</sub> models for heat transfer coefficients are published by several authors. The comparison of these models shows a good correspondence to the well known Gnielinsky model published in VDI (1994) (Rieberer, 1997b).

The left chart of Figure 2 shows a comparison of calculated (Index calc) with measured (Index meas) temperatures along the heat exchanger length ( $l$ ). The right chart shows the calculated local heat transfer coefficients ( $\alpha_{H_2O}$ ,  $\alpha_{CO_2}$ ) and the comparison of calculated local overall heat transfer coefficient ( $k_{calc}$ ) with the measured average value  $k_{meas}$  in the four ‘condenser’ sections.

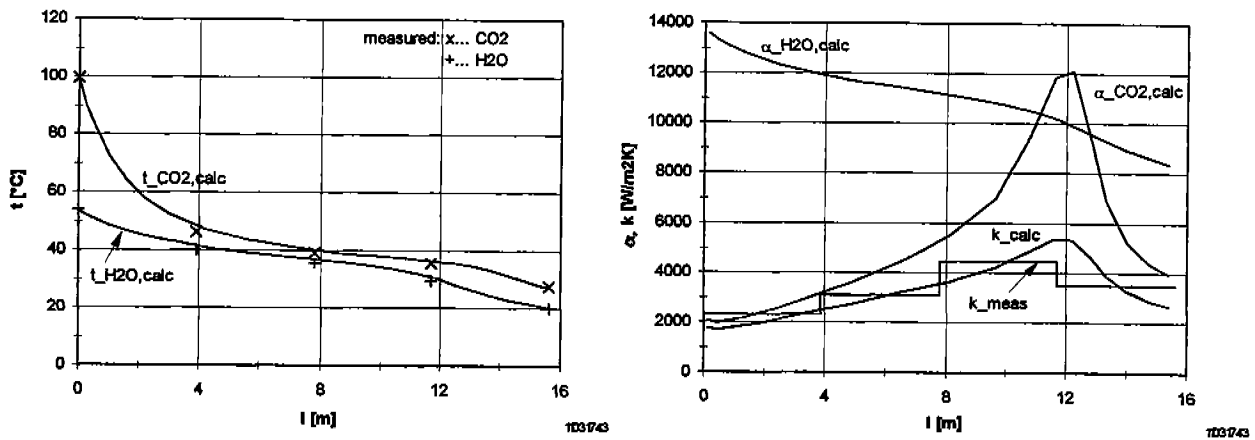


Figure 2: ‘Condenser’:  $M_{CO_2} = 0.0449$  kg/s,  $p_{CO_2,in} = 83.3$  bar;  $M_{H_2O} = 0.0787$  kg/s

As one can see, the deviations between calculated and measured values are negligible. Also the peak in the overall heat transfer coefficient is detected very well. The comparison of calculated pressure drop (according to VDI, 1994) with measured pressure drop is satisfactory too ( $\Delta p_{calc} = 1.0$  bar,  $\Delta p_{meas} = 0.9$  bar). (Remark: Caused by the large change of the properties along the heat exchanger, for the calculation a segmentation in approximately 15 ‘energy-equivalent’ parts was necessary.)

### 3.2 Evaporator

The calculation of the heat transfer coefficient and pressure drop at evaporation is more complex than for single-phase flow. The reasons are changing flow patterns along the tube length and the occurrence of (partial) dryout. Specific calculation models for CO<sub>2</sub> are not available in the literature. Most models available are developed for (H)CFCs. Bredeesen (1997) has published measurements of heat transfer coefficients and pressure drop gradients at evaporation of pure CO<sub>2</sub> in a horizontal tube. The heat transfer coefficient calculated according to VDI (1994) gives a good approximation to the measured values. The best fit of calculated to measured pressure drop gradients shows the model proposed by Thome (1997). (Rieberer, 1997b)

The left chart of Figure 3 shows the measured fluid temperatures as well as the measured wall temperatures along the heat exchanger length. The right chart shows the comparison of calculated local overall and local heat transfer coefficient of CO<sub>2</sub> according to VDI (1994) with the measured ones depending on the vapor quality ( $x$ ).

As can be seen, the calculated heat transfer coefficient has not even the same magnitude as the measured one! The measured <overall> heat transfer coefficient is in the range of 1800 W/m<sup>2</sup>K, the calculated one is approximately 70 % higher. Instead of an increasing CO<sub>2</sub> heat transfer coefficient - which is common in an annular flow regime - it is decreasing with  $x$ .

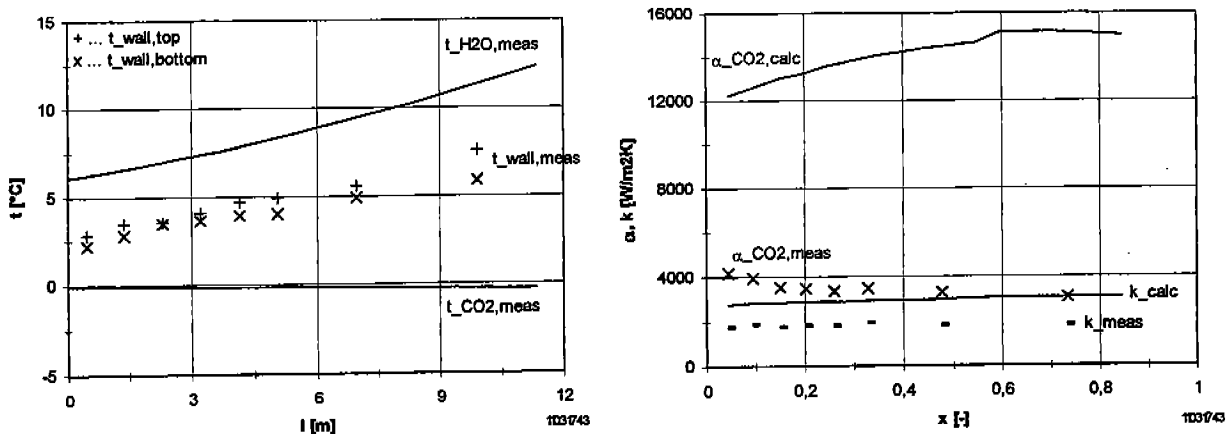


Figure 3: Evaporator:  $M_{CO_2}=0.0449\text{ kg/s}$ ,  $p_{CO_2,in}=34.8\text{ bar}$ ,  $x_{CO_2,in}=0.02$  ( $x_{CO_2,out}=0.87$ );  $M_{H_2O}=0.334\text{ kg/s}$

This can be explained by the dryout phenomenon. This theory is confirmed by the wall temperature measurements. Especially at higher vapor qualities the temperature on the top is ‘considerably’ higher than the temperature on the bottom. The reason for dryout might be the high specific heat flux - which is in the range of 20 000 W/m<sup>2</sup>, and/or the presence of oil (lubricant) in the cycle. An exact analysis has to be carried out. Nevertheless, the measured heat transfer coefficient of CO<sub>2</sub> under ‘realistic’ conditions is higher than those of most (H)CFCs. At evaporator inlet it is in the range of 4000 W/m<sup>2</sup>K, and at outlet it is 3000 W/m<sup>2</sup>K.

The comparison of calculated pressure drop according to Thome (1997) with measured pressure drop is more satisfactory ( $\Delta p_{calc} = 0.2\text{ bar}$ ,  $\Delta p_{meas} = 0.25\text{ bar}$ ).

### 3.3 Internal heat exchanger (IHx)

The heat transfer coefficient of the two-phase flow in the annulus (low pressure side, Index l.p.) is calculated by assuming a gaseous single-phase flow with a reduced mass flow rate of  $M_{red} = x \cdot M_{CO_2}$ , as the share of the liquid phase in total heat transfer will be very small due to a separation of the two phases in the annulus. The heat transfer coefficient of the high-pressure side (Index h.p.) is calculated according to the Gnielinsky correlation.

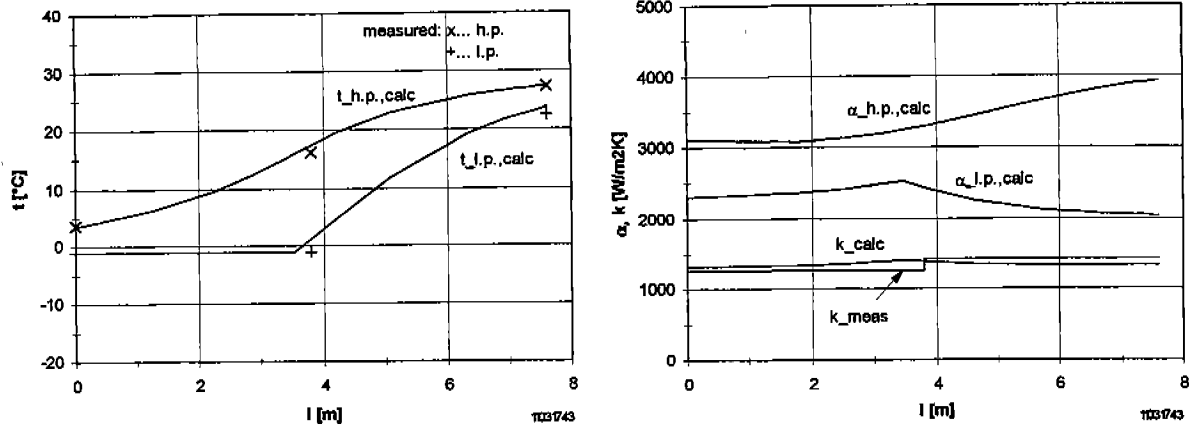


Figure 4: IHX:  $M_{CO_2} = 0.0449 \text{ kg/s}$ ,  $p_{CO_2,h.p.,in} = 82.3 \text{ bar}$ ;  $p_{CO_2,l.p.,in} = 33.8 \text{ bar}$ ,  $x_{CO_2,l.p.,in} = 0.87$

Figure 4 shows the results of the investigation. The deviation of calculated from measured values is small, especially in consideration of the two-phase flow, which is caused by the accumulator design (see next section). An overall heat transfer coefficient ( $k$ ) higher than  $1200 \text{ W/m}^2\text{K}$  is rather large, since heat is transferred from a quasi-liquid to a gaseous fluid. On both sides the calculated as well as the measured pressure drops are lower than  $0.3 \text{ bar}$ .

### 3.4 Accumulator

The design principle is explained in Chapter 2 and shown in Figure 5. The resulting vapor quality at the outlet can be calculated by using the Bernoulli equation and the theorem of momentum. For a certain mass flow rate and vapor quality at accumulator outlet, the conditions at accumulator inlet - and therefore at evaporator outlet - necessary for steady-state operation can be determined by means of the energy balance.

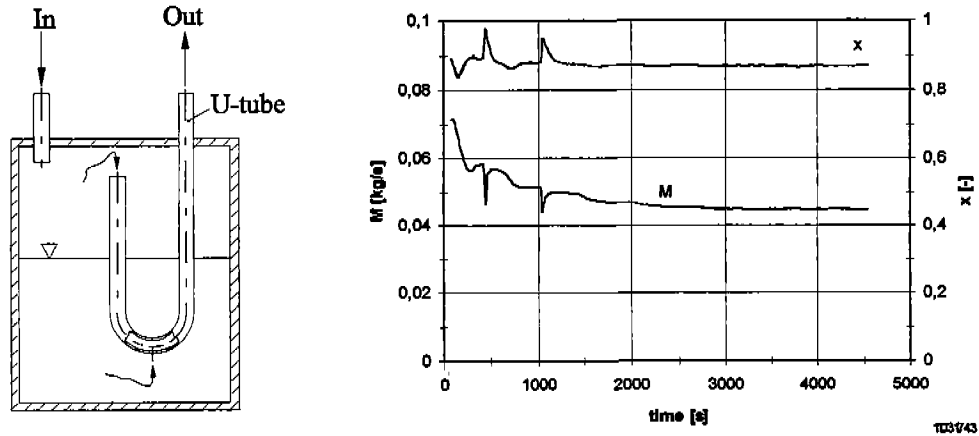


Figure 5: Accumulator, Design and Test Result

The diagram in Figure 5 shows the measured mass flow rate and outlet vapor quality. After start-up,  $x$  is constant at  $0.87$ . In the steady state-phase no remarkable influence of temperature ( $-10 \dots +10^\circ\text{C}$ ) or mass flow rate ( $0.04 \dots 0.065 \text{ kg/s}$ ) on the outlet vapor quality has been detected. The accuracy of the calculation is in the range of  $\Delta x = \pm 0.02$ .

### 3.5 Compressor Unit

Concerning the compressor power consumption ( $P_{\text{shaft}}$ ), following efficiencies are of importance:

- $\eta_{\text{is,over}} = P_{\text{isentropic}} / P_{\text{shaft}}$  (overall isentropic efficiency), and
- $\varepsilon = Q_{\text{loss}} / P_{\text{shaft}}$  (heat loss through the compressor envelope).

Measurements have shown that the power consumption was  $P_{\text{shaft}} = 2.65 \text{ kW}$ ,  $\eta_{\text{is,over}} \cong 0.75$ , and  $\varepsilon \cong 0.15$  for the example-cycle presented in this paper. Based on the measurements a compressor model is being developed.

Remark: The values given above were measured on the test rig at  $p_{\text{suction}} = 32 \text{ bar}$ ,  $p_{\text{discharge}} = 89 \text{ bar}$ , and a compressor speed of 795 rpm. In the efficiency numbers also losses in the suction and discharge line, in the filter, etc. are included. For a detailed analysis of the compressor see Süß (1997).

### 3.6 Overall System

The parameters given in the last sections - 'condenser':  $t_{\text{H}_2\text{O,in}} = 20^\circ\text{C}$ ,  $t_{\text{H}_2\text{O,out}} = 53.7^\circ\text{C}$ ,  $p_{\text{CO}_2,\text{in}} = 83.3 \text{ bar}$ ; evaporator:  $t_{\text{H}_2\text{O,in}} = 12.4^\circ\text{C}$  - result in a  $\text{COP} = Q_{\text{cond}} / P_{\text{shaft}} = 11.0 / 2.65 = 4.1$ . However, this value is not the maximum which is achievable with the  $\text{CO}_2$  heat pump water heater. Since the 'condenser' pressure of 83.3 bar is not the optimum, the cycle efficiency can be increased by better system control. A bigger potential for improvement is represented by the evaporator length: a longer evaporator will result in a higher evaporation temperature and therefore in a higher suction pressure. Furthermore, the pressure drops due to bends and fittings - for the measurement equipment - in the test rig are significant.

## 4 CONCLUSIONS

As measurements have shown, the calculation models used in the computer model HPSTAT deliver reliable values for the pressure drops and the heat transfer coefficients in the 'condenser' and the internal heat exchanger. The uncertainty in the evaporator is not fully solved. Therefore the present measurements are concentrated on the local heat transfer coefficient at various mass flow rates and evaporation temperatures. The influence of oil in the system is being investigated by means of an oil separator. The influence of the heat flux will be detected by using a larger heat exchanger.

Since this heat pump water heater is a first prototype, the components are not optimized. Anyway, the experience gained with it are the basis for future developments. Based on the experiments, calculation models are being modified, and an - economical - optimization of the heat exchangers as well as the development of a control system for a highly efficient and reliable heat pump will be possible.

Even this prototype shows that  $\text{CO}_2$  is an excellent refrigerant for heat pump water heaters, it is a 'natural' fluid without ODP and GWP, and it is a safety refrigerant.

## REFERENCES

- Bredesen A.M., Hafner A., Pettersen J., Neksa P., Aflekt K. (1997): 'Heat Transfer and Pressure Drop for In-tube Evaporation of  $\text{CO}_2$ ', IIR Conference: Heat Transfer Issues in 'Natural' Refrigerants, University of Maryland, USA.
- Neksa P., Rekstad H. (1997): 'CO<sub>2</sub> Heat Pump Prototype System- Experimental Results', IEA/IIR Workshop: CO<sub>2</sub> Technology in Refrigeration, Heat Pump & Air Conditioning Systems, Trondheim, Norway.
- Rieberer R., Kasper G., Halozan H. (1997a): 'CO<sub>2</sub> - A Chance For Once-Through Heat Pump Heaters', IEA/IIR Workshop: CO<sub>2</sub> Technology in Refrigeration, Heat Pump & Air Conditioning Systems, Trondheim, Norway.
- Rieberer R., Halozan H. (1997b): 'Design of Heat Exchangers for CO<sub>2</sub>-Heat Pump Water Heaters', IIR Conference: Heat Transfer Issues in 'Natural' Refrigerants, University of Maryland, USA.
- Süß J., Kruse H. (1997): 'Design Criteria of CO<sub>2</sub>-Compressors for Vapor Compression Cycles', IIR Conference: Heat Pump Systems, Energy Efficiency, and Global Warming, Linz, Austria.
- Thome J.R. (1997): 'Refrigeration Heat Transfer', Course notes, GRETh/CEA, Grenoble, France.
- VDI (1994): 'VDI Wärmeatlas: Berechnungsblätter für den Wärmeübergang', 7. Auflage, VDI Verlag, Düsseldorf, Germany.